

# Anomalous Structure and Scaling of Ring Polymer Brushes

Daniel Reith,<sup>1,\*</sup> Andrey Milchev,<sup>2</sup> Peter Virnau,<sup>1</sup> and Kurt Binder<sup>1</sup>

<sup>1</sup> *Institut für Physik, Johannes Gutenberg-Universität*

*D-55099 Mainz, Staudinger Weg 7, Germany*

<sup>2</sup>*Institute of Physical Chemistry, Bulgarian Academy of Sciences, Sofia 1113, Bulgaria*

## Abstract

A comparative simulation study of polymer brushes formed by grafting at a planar surface either flexible linear polymers (chain length  $N_L$ ) or (non-catenated) ring polymers (chain length  $N_R = 2N_L$ ) is presented. Two distinct off-lattice models are studied, one by Monte Carlo methods, the other by Molecular Dynamics, using a fast implementation on graphics processing units (GPUs). It is shown that the monomer density profiles  $\rho(z)$  in the  $z$ -direction perpendicular to the surface for rings and linear chains are practically identical,  $\rho_R(2N_L, z) = \rho_L(N_L, z)$ . The same applies to the pressure, exerted on a piston at high  $z$ , as well. While the gyration radii components of rings and chains in  $z$ -direction coincide, too, and increase linearly with  $N_L$ , the transverse components differ, even with respect to their scaling properties:  $R_{gxy}^{(L)} \propto N_L^{1/2}$ ,  $R_{gxy}^{(R)} \propto N_L^{0.4}$ . These properties are interpreted in terms of the statistical properties known for ring polymers in dense melts.

PACS numbers: 82.35.Lr, 61.46.-w, 61.25.Hq

---

\*Electronic address: reithd@uni-mainz.de

## I. INTRODUCTION AND MOTIVATION

Dense layers of macromolecules grafted by special chemical groups to non-adsorbing substrates have found enormous interest recently (for reviews see [1–6]) in view of numerous applications: colloid stabilization [7]; improvement of lubrication properties [2], also in a biological context [8], creation of functional surfaces with switchable properties [9], improvement of drug biocompatibility [10], microfluidic devices for biomolecule separation [11], etc. The theoretical understanding of the (often unexpected) properties of polymer brushes, due to an interesting interplay of monomer-monomer and monomer-solvent interactions and the entropic forces resulting from the confinement of macromolecular conformations, has been a longstanding challenge as well (e.g. [1, 4, 6, 12–18]).

To the best of our knowledge, all this research has focused on the grafting of linear polymers by a special end-group at one chain end; only as one exception the formation of “loop brushes” (where both chain ends are grafted to the substrate) has been considered [19]. In the latter case, although the chains are permanently entangled (forming a “catenated” network-like structure), the brush properties are found to differ at best marginally from those of brushes with free ends [19].

In recent years, there has been a great interest in the properties of polymer melts formed from non-catenated ring polymers [20–40]. Both synthetic polymers (such as polyethylene or polystyrene [22]) and biopolymers such as DNA can be prepared as closed rings, and are of great interest as model system, to understand such diverse problems as polymer melt dynamics when the standard reptation mechanism (that needs chain ends [41]) is eliminated [20, 21, 23], and the organization of DNA in the cell nucleus [37, 42–45]. Note that most of the short genomes as well as plasmids are circular [46, 47] and also actin can self-assemble into rings [48]. Ring polymers under various kinds of confinement are also under discussion in this biological context (see, e.g., [49, 50]).

It is a challenging problem to understand the conformation of ring polymers (both with respect to single collapsed rings [51] and confined rings [49, 50, 52] and rings in melts [20–40]). One famous picture is that collapsed rings (as well as rings in a melt) are “crumpled globules”, where each subchain of the loop is condensed in itself, and the fractal dimension of the object is  $d_f = 3$ . Hence the gyration radius scales like a compact globule,  $R_g \propto N_R^{1/3}$ ,  $N_R$  being the number of (effective) monomers in the ring polymer (hereafter, referred to

as ring length). However, when one hypothesizes that the structure of a ring polymer in a melt resembles a “lattice animal” (where every bond of the lattice is traversed by the polymer twice, in opposite directions) one predicts [26]  $R_g \propto N_R^{2/5}$ . The evidence from both experiment and simulations on this issue has been discussed controversially over decades, and only recently a resolution seems to emerge [36, 37, 39, 40]: the ring polymers in melts behave like lattice animals for intermediate ring lengths but then crossover to crumpled globule-like structures for very long rings. Recall that both powers are substantially different from the law seen for melts of linear polymers, where a scaling like for gaussian chains occurs,  $R_g \propto N_L^{1/2}$  [53]. We also stress that a (hypothetical) melt of ring polymers where the rings were free to cross each other, topological non-crossability constraints being “switched off”, would have trivial Gaussian statistics [53] as well.

In the present paper, we ask what happens when ring polymers are grafted to a planar substrate by special groups at a single monomer. It is well known that for a polymer brush formed from linear chains at large enough grafting densities  $\sigma_g$  strongly stretched polymer configurations result while in the lateral direction the chains behave ideal [1, 6]

$$R_{gz}^{(L)} \propto \sigma_g^{1/3} N_L, R_{gxy}^{(L)} \propto \sigma_g^{-1/12} N_L^{1/2} \quad , \quad (1)$$

where  $N_L$  is the number of (effective) monomers in the linear polymer. The prefactor describing the  $\sigma_g$ -dependence can already be understood from the simple Alexander-de Gennes [12, 13] blob picture, describing a chain by a string of blobs of diameter  $d \propto \sigma_g^{-1/2}$ , each blob containing  $g = d^{5/3}$  monomers, taking  $n = N_L/g$  steps in the  $z$ -direction perpendicular to the substrate while the typical excursion parallel to the substrate is of order  $\sqrt{nd}$ . The self-avoiding walk statistics inside a blob,  $d \propto g^\nu$  with  $\nu = 3/5$  is, of course, implicitly included in this argument. By comparing our simulation results for ring polymers with ring lengths  $N_R = 2 N_L$  of otherwise identical linear polymers forming a brush, at  $\sigma_{g,R} = \sigma_{g,L}/2$  (to keep the number of effective monomers strictly the same), we are able to clarify the effect of the topological interaction on the rings in this situation. We shall show indeed certain characteristic differences between ring brushes and linear brushes, which can be traced back to these topological effects.

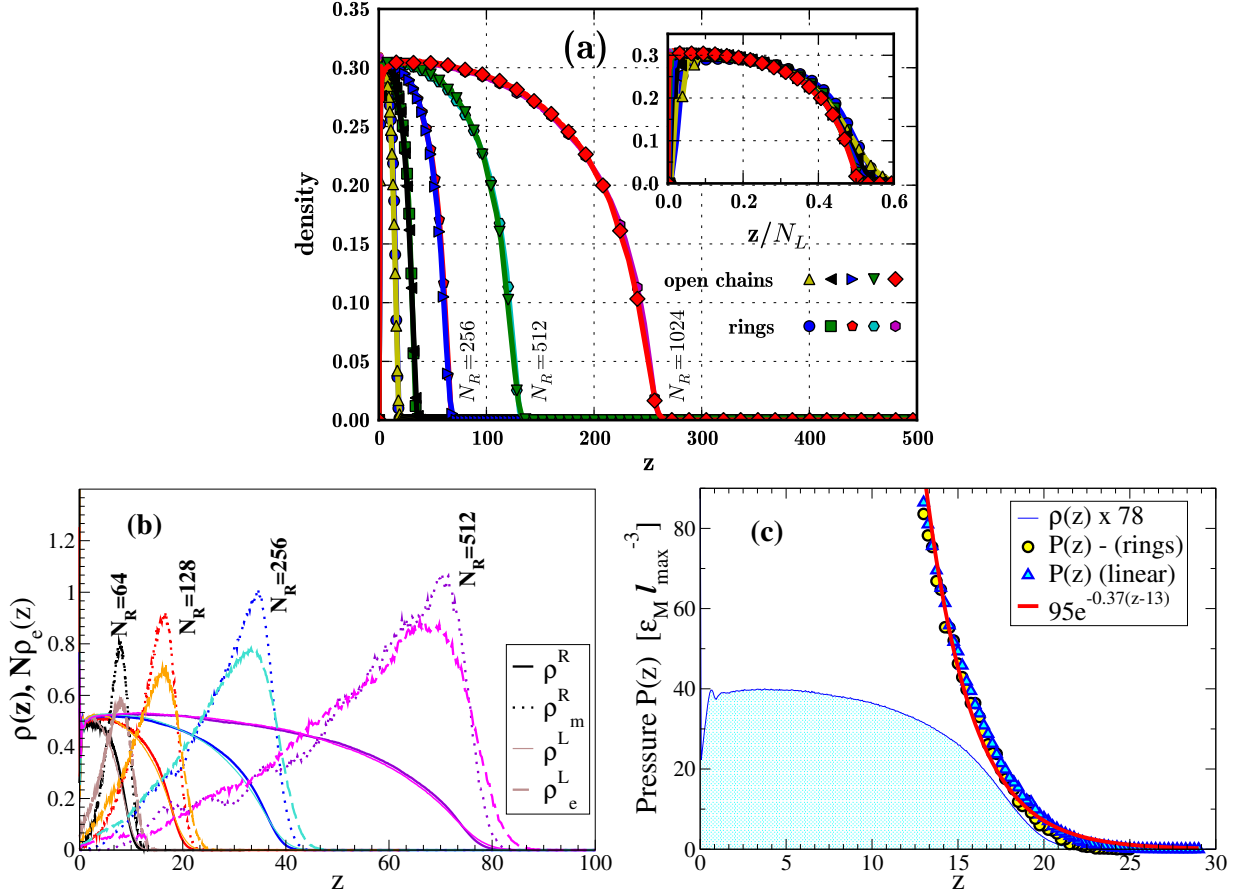


FIG. 1: (a) Density profiles along the  $z$ -direction for rings and linear chains of different length (MD data). The density profiles scale linearly with the chain length for linear chains respectively half the length for rings. In the inset the curves collapse using this scaling relation. (b) Total monomer number density  $\rho(z)$ , and end-monomers,  $\rho_e(z)$ , respectively, middle-monomer density  $\rho_m(z)$  from MC data. Here  $\sigma_g^R = 0.0625$  (rings) and  $\sigma_g^L = 0.125$  (linear chains). (c) Pressure, exerted by the polymer brush of rings (circles), and linear chains (triangles) on a piston at distance  $z$  from the grafting plane - MC data for  $\sigma_g^R = 0.0625$  (rings) and  $\sigma_g^L = 0.125$  (linear chains). Here  $N_R = 128$ ,  $N_L = 64$ . The density profile is included for comparison.

## II. MODELS AND SIMULATION TECHNIQUES

We always choose  $L \times L$  grafting plane and periodic boundary conditions in  $x, y$  directions. Chains are grafted at a grafting density  $\sigma_{g,L} = 0.125$  for the linear chains with the range parameter  $\sigma$  of the Weeks-Chandler-Andersen (WCA) potential that describes the

interaction between effective monomers in our MD simulations as unit of length

$$U_{WCA}(r) = 4\varepsilon \left[ (\sigma/r)^{12} - (\sigma/r)^6 + \frac{1}{4} \right], \quad r < r_c = 2^{1/6}\sigma \quad . \quad (2)$$

$r$  being the distance between any pair of monomers (bonded or nonbonded ones).  $U_{WCA}(r \geq r_c) = 0$ , so the potential is purely repulsive. As is standard [4, 54] bonded monomers interact with the finitely extensible nonlinear elastic (FENE) potential in addition,

$$U_{\text{FENE}}(r) = -0.5kR_0^2 \ln[1 - (r/R_0)^2] \quad , \quad r < R_0 \quad , \quad (3)$$

where  $U_{\text{FENE}}(r > R_0) \equiv 0$ . Parameters chosen are  $\varepsilon = 1$ , temperature  $T = 1.0 \varepsilon/k_B$  and  $k = 30$ ,  $R_0 = 1.5$ . The mass of the particles  $m = 1$  as well, so the MD time unit is  $\tau = \sigma/\sqrt{m/\varepsilon} = 1$  as well. MD runs were carried out on GPUs using the HooMD Blue r3574 code [55]. Note that due to the use of GTX480 GPUs, a speedup factor of roughly 70 in comparison to a run on a single i7 CPU core for the present application is obtained. We use a standard dissipative particle dynamics (DPD) thermostat [56] with parameters  $\gamma = 0.5$ ,  $r_{\text{cut}} = 1.25 \cdot 2^{1/6}$ , and integration time step  $\delta t = 0.005$ . The grafting of the first monomer to the substrate site in the  $z = 0$  substrate plane is realized by the same FENE potential as in Eq. (3). Note that the linear dimension  $L$  is adjusted such that we always have either  $\mathcal{N} = 51200$  or  $\mathcal{N} = 102400$  effective monomers in the system, for chain lengths  $N_L = 16, 32, 64, 128, 256$  and  $512$ , respectively (recall  $N_R = 2N_L$ ,  $\sigma_{g,R} = \sigma_{g,L}/2$  throughout). For the longest chains, an equilibration time of  $\tau_{\text{eq}} \approx 2.1 \cdot 10^8$  was needed.

MC simulations were done using a somewhat different off-lattice model that we describe in the following. Of course, the motivation for choosing two different models is to confirm the universality of our results, which should not depend on irrelevant simulation details, but are rather generic. We employ a model of flexible polymer chains, each polymer consisting of  $N_L$  or  $N_R$  beads connected by anharmonic springs. These springs are defined by the FENE potential, Eq. (3), albeit with  $r = \ell - \ell_0$ . Thus,  $\ell$  is the bond length, which can vary between  $\ell_{\text{min}} < \ell < \ell_{\text{max}}$ , and has the equilibrium value  $\ell_0 = 0.7$ , while  $\ell_{\text{max}} = \ell_0 + R_0$ ,  $\ell_{\text{min}} = \ell_0 - R_0$ , and  $R_0 = 0.3$ . With these parameters  $\ell_{\text{max}} = 1$  is the unit of the length. A short-range Morse potential is used to describe non-bonded interactions,

$$U_M(r) = \varepsilon_M \exp[-2(r - r_{\text{min}})] - 2 \exp[-x(r - r_{\text{min}})], \quad (4)$$

with  $\varepsilon_M = 1$ ,  $r_{\text{min}} = 0.8$ ,  $\alpha = 24$ . Since for this model the  $\theta$ -temperature is  $k_B\Theta \approx 0.62$ , in the present study we work at temperature  $k_B\Theta = 1.0$ , and are thus in the ‘‘good solvent’’

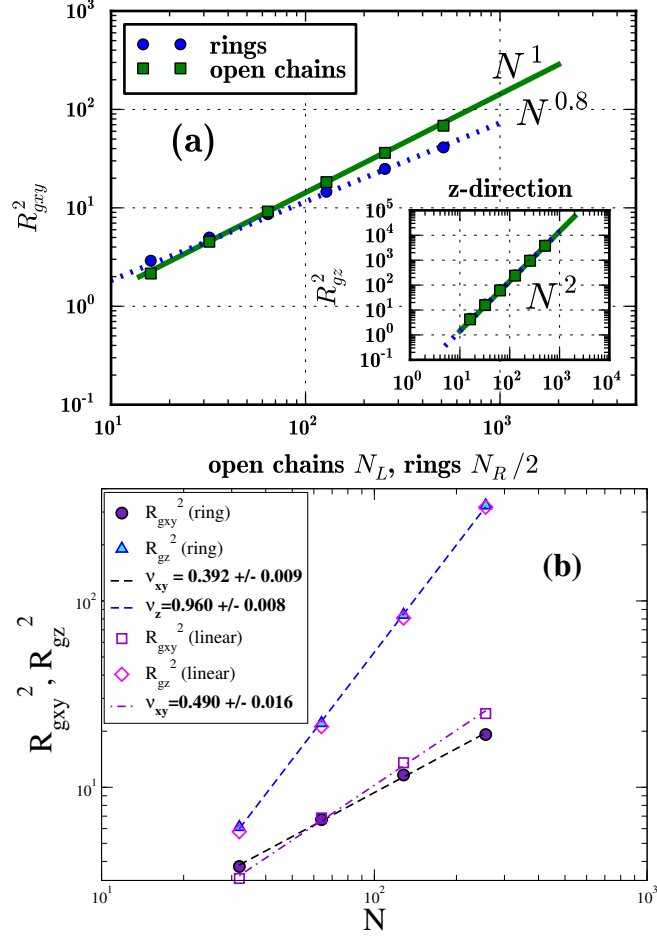


FIG. 2: (a) Squared radius of gyration (MD) parallel to the grafting plane on double logarithmic scale  $R_{gxy}^2 = R_{gx}^2 + R_{gy}^2$  against chain length  $N_L$  (linear chains) and  $N_R/2$  (rings), respectively. Inset - Scaling of the squared radius of gyration  $R_{gz}^2$  perpendicular to the grafting plane. The scaling prefactors differ by a factor of 4 between linear chains and rings. (b) The same from MC data for  $\sigma_g^R = 0.0625$  (rings) and  $\sigma_g^L = 0.125$  (linear chains).

regime. The Monte Carlo procedure consists of local displacements of the monomers only, which are accepted according to the usual Metropolis criterion. Typically, systems containing 32768 monomers are simulated about  $6 \div 10 \times 10^6$  MCS after equilibration, whereby various quantities of interest are sampled.

### III. RESULTS AND DISCUSSION

One of the central static properties of polymer brushes is the density profile  $\rho(z)$  of monomers in the  $z$ -direction perpendicular to the brush (Fig. 1a, b). A striking finding is that for both models, the density profiles of linear chains and rings are identical, within statistical errors (which are larger for the MC calculation, due to the much smaller statistical effort). The insert of Fig. 1a shows the profiles rescaling  $z$  by  $N_L$ , to demonstrate that the data converge to the strong stretching limit. For small  $N_L$  there are oscillations for small  $z$  and a “finite size tail” for large  $z$ : these “corrections to scaling” become negligible in the limit of very long chains. However, the variation of  $\rho(z)$  near the brush height  $h$  (where  $\rho(z)$  vanishes for large  $N_L$ ) is somewhat steeper than expected from the strong stretching limit of self-consistent field theory [14, 15], which would imply that  $\rho(z)/\rho(0) = 1 - (z/h)^2$ : the latter result requires that the density inside of the blobs does not exceed the semi-dilute regime [53]. However, one should note that melt densities would be (in our units [54]) of order  $\rho \approx 1$  for the MD model and  $\rho \approx 2$  for the MC model. It is clear that our choice of parameters (leading to  $\rho(0) \approx 0.3$ , see Fig. 1a) corresponds to the regime of a rather concentrated solution rather than a semidilute solution (remember that Eq. 2 accounts for the effects of a good solvent only implicitly rather than explicitly, of course).

Fig. 1b also includes the distribution of free chains ends (for the linear chains) and of the mid-monomers with index  $i = N_R/2$  for the rings (which have  $N_R = 2N_L$  monomers, monomers being labeled consecutively along the ring,  $i = 1$  being the grafted monomer). While according to the picture of the “Alexander brush” [12]  $\rho_e(z) \propto \delta(z - h)$ , all end monomers need to be at the brush end, the actual distribution  $\rho_e(z)$  shows that the ends (or mid-monomers in the case of rings, respectively) can be anywhere in the brush (although only few are near the grafting plane, since  $\rho_e(z) \propto z$  for  $z \ll h$  [14]). It is interesting to notice that in  $\rho_e(z)$  there are slight but systematic differences between linear chains and rings: for the latter the distributions are significantly more sharply peaked, and the tail towards large  $z$  is less pronounced. This is not surprising, of course, since the mid-monomer is bound by two strands rather than a single one. In Fig. 1c we show the pressure, exerted by a brush or ring (circles), or linear polymers (triangles) on a piston at height  $z$  above the grafting plane. Evidently, the pressure closely follows the monomer density profile at the brush tail, whereby one hardly detects any difference between rings and linear chains.

A very interesting behavior results when we examine the linear dimensions of individual chains, however (Fig. 2a, 2b). While the  $z$ -components of the mean square gyration radii in  $z$ -directions  $\langle R_{gz}^2 \rangle$  for linear chains and rings coincide precisely, the transverse components differ significantly, indicating a different power law,

$$\langle R_{gxy}^2 \rangle \propto N \quad (\text{linear chains}), \quad \langle R_{gxy}^2 \rangle \propto N^{0.8} \quad (\text{rings}) \quad . \quad (5)$$

While the first of these equations is expected (Eq. (1)), the second is not. Surprisingly, our data coincide with the theoretical prediction for lattice animals ( $\nu = 2/5$ ) [26] over a full decade in  $N$ , for both models. For very small  $N$ , deviations occur, as expected, but indications for a crossover to the “crumpled globule” exponent [51] ( $\nu = 1/3$ ) are not seen, unlike the case of bulk polymer melts [30–40]. Of course, while it is conceivable that another crossover could occur for much larger ring lengths, it is not really clear that one should expect this: after all, the  $z$ -components of the grafted chains in the brush are strongly stretched,  $\langle R_{gz}^2 \rangle \propto N^2$ , while in a ring polymer melt all components  $R_{gx}^2$ ,  $R_{gy}^2$  and  $R_{gz}^2$  scale in the same way. Due to this strong anisotropy, it remains unclear if the transverse components  $R_{gxy}^2$  of the chains in a ring polymer brush should exhibit the same scaling as chains in a ring polymer melt. The fact that the mean-square gyration radii in  $z$ -direction,  $\langle R_{gz}^2 \rangle$ , for linear chains and rings (under equivalent conditions,  $N_R = 2N_L$ ,  $\sigma_g^R = \sigma_g^L/2$ ) coincide, while the transverse components are so different in both cases, should not be mistaken as a proof that  $z$ -components and transverse components are decoupled, however. When one compares the full probability distributions  $P(R_{gz}^2)$  for rings and linear chains, one does see characteristic differences: for very small  $R_{gz}^2$ , the distribution in the case of rings has much more weight than it has for linear chains (Fig. 3). Of course, this finding does not contradict Figs. 2a, 2b, since the region of very small  $R_{gz}^2$  makes only negligibly small contributions to  $\langle R_{gz}^2 \rangle$ .

#### IV. CONCLUDING SUMMARY

In this letter, we consider a new class of polymer brushes, formed by densely grafted ring polymers to a flat substrate surface. We demonstrate that the transverse configuration of such grafted rings differs substantially from corresponding linear chains (Fig. 2) although collective properties (such as the average density profiles of the monomers (Figs. 1a,b) or the pressure exerted by the brush on a compressing wall (1c)) basically do not differ at all.



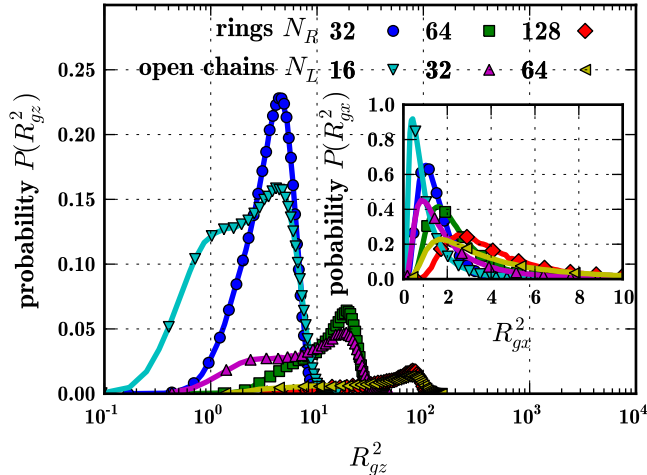


FIG. 3: Normalized probability distributions of  $R_{gz}^2$  for rings and linear chains of different length  $N$ . The shoulders in the probability distribution of the open chains towards lower values of  $R_{gz}^2$  indicate that this distribution is non-gaussian - there is a higher probability of finding compact configurations of linear chains as compared to rings of double length. *Inset*: Normalized probability distribution of the squared radius of gyration in x-direction parallel to the grafting plane  $R_{gx}^2$ .

An intriguing question is the interpretation of our findings in terms of geometric properties of chain versus ring conformations (Fig 4 shows some illustrative snapshots). In the corresponding problem of non-catenated rings forming dense melts, one associates a  $R_g \sim N_R^{2/5}$  variation with lattice animal like conformations (while for very large ring-lengths  $N_R$  one rather finds [39] crumpled globules, leading to  $R_g \sim N_R^{1/3}$ ). Obviously, the projections of monomer positions into the xy-plane for rings (Fig. 4) are fairly compact, while the corresponding projections for linear chains are random walk-like.

An intriguing question is what phenomena are affected by these different conformations of rings (rather than linear chains) forming a polymer brush. Presumably, for instance, the dynamics of free (linear) chains from a solution or melt flowing past a ring polymer brush will be very different. The interaction with nanoparticle inclusions, that involves the deformation of chains (or rings) surrounding the nanoparticle would be rather different. All such questions remain to be explored also.

Of course, it would be very nice if guidance from analytical theory were available to understand the differences between ring polymer brushes and ordinary brushes formed from linear polymers, as we have found in our studies. However, none of the well-established

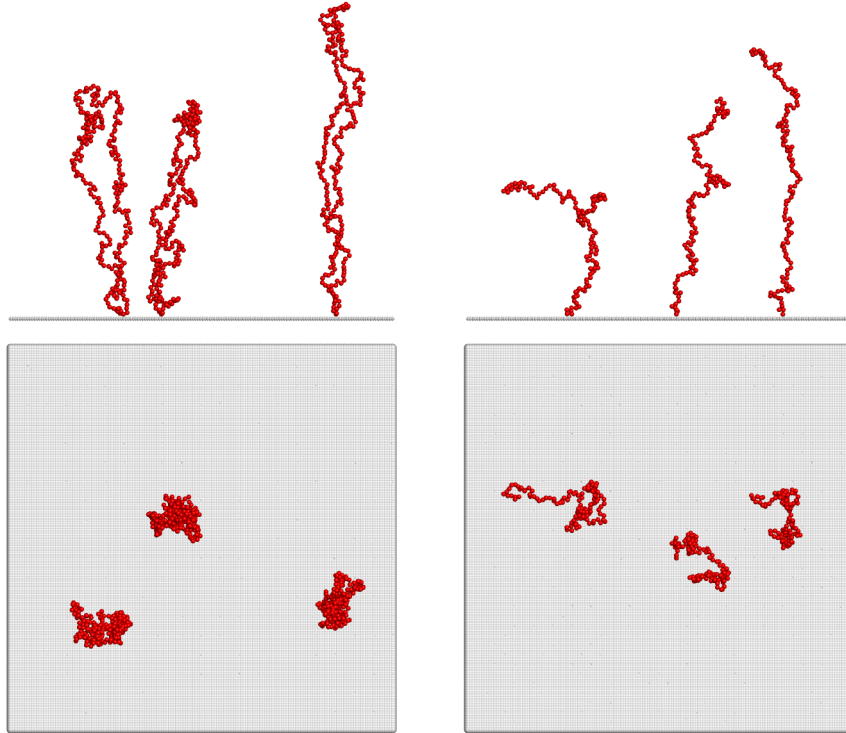


FIG. 4: Configurations from Molecular dynamics simulations to illustrate the conformational differences between loops and open chains: 3 out of 400 loops of ring length  $N_R = 256$  (*left*) and 3 out of 800 open chains of chain length  $N_L = 128$  (*right*) are displayed. The rings and the open chains are grafted on a  $80 \times 80$  grafting plane. The overall number of monomers is 102400 per system.

approaches (self-consistent field theory [14–16], density functional-type theories [3, 57], etc) can take the topological differences between catenated and non-catenated rings into account: none of the theories could hence predict any of the differences that we have found here. Also experimental studies of this problem (ideally one might consider neutron scattering from deuterated rings in a protonated ring polymer brush) are a great challenge.

### Acknowledgments

We thank the Deutsche Forschungsgemeinschaft (DFG) for partial support under grant number SFB 625/A17 (D.R.) and BI 314/23 (A.M.) and are grateful to K. Kremer for sending preprints of Refs. 39,40 and stimulating discussions. Computing time on the GPU cluster of the Center for Computational Sciences Mainz at the ZDV Mainz are gratefully

acknowledged, too.

---

- [1] A. Halperin, M. Tirrell, and T. Lodge, *Adv. Polym. Sci.* **100**, 31 (1992).
- [2] J. Klein, *Annu. Rev. Mater. Sci.* **26**, 581 (1996).
- [3] I. Szleifer and M. A. Carignano, *Adv. Chem. Phys.* **94**, 165 (1996).
- [4] G. S. Grest, *Adv. Polym. Sci.* **138**, 149 (1999).
- [5] R. C. Advincula, W. J. Brittain, K. C. Caster, and J. R uhe, eds., *Polymer brushes* (Wiley-VCH, Weinheim, 2004).
- [6] K. Binder, T. Kreer, and A. Milchev, *Soft Matter* p. in press (2011).
- [7] D. Napper, *Polymeric Stabilization of Colloidal Dispersions* (Academic, London, 1983).
- [8] J. Klein, *Science* **323**, 47 (2009).
- [9] H. Merlitz, G.-L. He, C.-X. Wu, and J.-U. Sommer, *Phys. Rev. Lett.* **102**, 115702 (2009).
- [10] G. Storm, *Adv. Drug. Deliv. Rev.* **17**, 31 (1995).
- [11] A.-J. Wang, J.-J. Xu, and H.-Y. Chen, *J. Chromatogr. A* **1147**, 120 (2007).
- [12] S. Alexander, *J. Phys.* **38**, 977 (1977).
- [13] P. G. de Gennes, *Macromolecules* **13**, 1069 (1980).
- [14] S. T. Milner, T. a. Witten, and M. E. Cates, *Macromolecules* **21**, 2610 (1988).
- [15] E. B. Zhulina, O. V. Borisov, V. a. Pryamitsyn, and T. M. Birshtein, *Macromolecules* **24**, 140 (1991).
- [16] R. Netz and M. Schick, *Macromolecules* **31**, 5105 (1998).
- [17] T. Kreer, S. Metzger, M. M uller, K. Binder, and J. Baschnagel, *J. Chem. Phys.* **120**, 4012 (2004).
- [18] A. Galuschko, L. Spirin, T. Kreer, A. Johnner, C. Pastorino, J. Wittmer, and J. Baschnagel, *Langmuir* **26**, 6418 (2010).
- [19] F. Yin, D. Bedrov, G. D. Smith, and S. M. Kilbey, *J. Chem. Phys.* **127**, 084910 (2007).
- [20] J. Roovers, *Macromolecules* **21**, 1517 (1988).
- [21] G. B. McKenna, B. J. Hostetter, N. Hadjichristidis, L. J. Fetters, and D. J. Plazek, *Macromolecules* **22**, 1834 (1989).
- [22] S. Gagliardi, V. Arrighi, R. Ferguson, a. C. Dagger, J. a. Semlyen, and J. S. Higgins, *J. Chem. Phys.* **122**, 064904 (2005).

- [23] D. Kawaguchi, K. Masuoka, A. Takano, K. Tanaka, T. Nagamura, N. Torikai, R. M. Dalglish, S. Langridge, and Y. Matsushita, *Macromolecules* **39**, 5180 (2006).
- [24] M. Kapnistos, M. Lang, D. Vlassopoulos, W. Pyckhout-Hintzen, D. Richter, D. Cho, T. Chang, and M. Rubinstein, *Nature Mater.* **7**, 997 (2008).
- [25] S. Nam, J. Leisen, V. Breedveld, and H. W. Beckham, *Macromolecules* **42**, 3121 (2009).
- [26] M. Cates and J. Deutsch, *J. Phys.* **47**, 2121 (1986).
- [27] M. Müller, J. Wittmer, and M. Cates, *Phys. Rev. E.* **53**, 5063 (1996).
- [28] S. Brown and G. Szamel, *J. Chem. Phys.* **108**, 4705 (1998).
- [29] S. Brown and G. Szamel, *J. Chem. Phys.* **109**, 6184 (1998).
- [30] M. Müller, J. P. Wittmer, and J.-L. Barrat, *Europhys. Lett.* **52**, 406 (2000).
- [31] M. Müller, J. Wittmer, and M. Cates, *Phys. Rev. E.* **61**, 4078 (2000).
- [32] S. Brown, T. Lenczycki, and G. Szamel, *Phys. Rev. E.* **63**, 3 (2001).
- [33] K. Hur, R. G. Winkler, and D. Y. Yoon, *Macromolecules* **39**, 3975 (2006).
- [34] J. Suzuki, A. Takano, and Y. Matsushita, *J. Chem. Phys.* **129**, 034903 (2008).
- [35] J. Suzuki, A. Takano, T. Deguchi, and Y. Matsushita, *J. Chem. Phys.* **131**, 144902 (2009).
- [36] T. Vettorel, S. Y. Reigh, D. Y. Yoon, and K. Kremer, *Macromol. Rapid Commun.* **30**, 345 (2009).
- [37] T. Vettorel, A. Y. Grosberg, and K. Kremer, *Phys. Biol.* **6**, 025013 (2009).
- [38] K. Hur, C. Jeong, R. G. Winkler, N. Lacevic, R. H. Gee, and D. Y. Yoon, *Macromolecules* **44**, 2311 (2011).
- [39] J. D. Halverson, W. B. Lee, G. S. Grest, A. Y. Grosberg, and K. Kremer (2010).
- [40] J. D. Halverson, W. B. Lee, G. S. Grest, A. Y. Grosberg, and K. Kremer (2010).
- [41] M. Doi and S. Edwards, *The Theory of Polymer Dynamics* (Oxford University Press, Oxford, 1986).
- [42] H. Kimura and P. Cook, in *Nuclear dynamics: molecular biology and visualization of the nucleus* (Springer Japan, 2007).
- [43] K. J. Meaburn and T. Misteli, *Nature* **445**, 379 (2007).
- [44] J. Dorier and A. Stasiak, *Nucleic Acids Res.* **37**, 6316 (2009).
- [45] E. Lieberman-Aiden, N. L. van Berkum, L. Williams, M. Imakaev, T. Ragozy, A. Telling, I. Amit, B. R. Lajoie, P. J. Sabo, M. O. Dorschner, et al., *Science* **326**, 289 (2009).
- [46] B. Alberts, A. Johnson, P. Walter, J. Lewis, M. Raff, and K. Roberts, *Molecular Biology of*

*the Cell* (Taylor & Francis, London, 2008), 5th ed.

- [47] G. Witz, K. Rechendorff, J. Adamcik, and G. Dietler, *Phys. Rev. Lett.* **101**, 3 (2008).
- [48] T. Sanchez, I. M. Kubic, and Z. Dogic, *Phys. Rev. Lett.* **104**, 65 (2010).
- [49] Y. Liu and B. Chakraborty, *Phys. Biol.* **5**, 026004 (2008).
- [50] M. Fritsche and D. W. Heermann (2011).
- [51] A. Grosberg, S. Nechaev, and E. Shakhnovich, *J. Phys.* **49**, 2095 (1988).
- [52] K. Ostermeir, K. Alim, and E. Frey, *Phys. Rev. E.* **81**, 1 (2010).
- [53] P. de Gennes, *Scaling Concepts in Polymer Physics* (Cornell University Press, Ithaca, 1979).
- [54] K. Kremer and G. S. Grest, *J. Chem. Phys.* **92**, 5057 (1990).
- [55] J. Anderson, C. Lorenz, and A. Travesset, *J. Comput. Phys.* **227**, 5342 (2008).
- [56] T. Soddemann, B. Dünweg, and K. Kremer, *Phys. Rev. E.* **68**, 1 (2003).
- [57] S. A. Egorov, *J. Chem. Phys.* **129**, 064901 (2008).